Transgenic Res (2016) 25:533–544
DOI 10.1007/s11248-016-9941-9

BRIEF COMMUNICATION

Hypomorphic phenotype of *Foxn1* gene-modified rats by CRISPR/Cas9 system

Teppei Goto · Hiromasa Hara · Hiromitsu Nakauchi · Shinichi Hochi · Masumi Hirabayashi

Received: 13 July 2015 / Accepted: 19 February 2016 / Published online: 2 March 2016

Abstract The *Foxn1* gene is known as a critical factor for the differentiation of thymic and skin epithelial cells. This study was designed to examine the phenotype of *Foxn1*-modified rats generated by the CRISPR/Cas9 system. Guide-RNA designed for first exon of the *Foxn1* and mRNA of Cas9 were co-injected into the pronucleus of Crlj:WI zygotes. Transfer of 158 injected zygotes resulted in the birth of 50 offspring (32 %), and PCR identified five (10 %) as *Foxn1*-edited. Genomic sequencing revealed the deletion of 44 or 60 bp from and/or insertion of 4 bp into the *Foxn1* gene in a single allele. The number of T-cells in the peripheral blood lymphocytes of mutant rats decreased markedly. While homozygous deleted mutant rats had no thymus, the mutant rats were not completely hairless and showed normal performance in delivery and nursing. Splicing variants of the indel-mutation in the *Foxn1* gene may cause hypomorphic allele, resulting in the phenotype of thymus deficiency and incomplete hairless. In conclusion, the mutant rats in *Foxn1* gene edited by the CRISPR/Cas9 system showed the phenotype of thymus deficiency and incomplete hairless which was characterized by splicing variants.

Keywords CRISPR/Cas9 · *Foxn1* · Knock-out rat · Splicing variant · Thymus deficiency

Electronic supplementary material The online version of this article (doi:10.1007/s11248-016-9941-9) contains supplementary material, which is available to authorized users.

T. Goto · H. Hara · M. Hirabayashi (✉)
Section of Mammalian Transgenesis, Center for Genetic Analysis of Behavior, National Institute for Physiological Sciences, 5-1 Higashiyama, Myodaiji-cho, Okazaki, Aichi 444-8787, Japan
e-mail: mhirarin@nips.ac.jp

H. Nakauchi
Japan Science Technology Agency, ERATO, Nakauchi Stem Cell and Organ Regeneration Project, Minato-ku, Tokyo, Japan

H. Nakauchi
The Institute of Medical Science, The University of Tokyo, Minato-ku, Tokyo, Japan

S. Hochi
Faculty of Textile Science and Technology, Shinshu University, Ueda, Nagano, Japan

Introduction

Targeted mutations can be induced by the use of genome editing tools, not only in cultured cells and model organisms, but also in higher plants and mammalian species. The genome editing tools, which can induce mutations through DNA double-strand breaks and error-prone repair by non-homologous end joining, include zinc-finger nucleases (ZFNs), transcription activator-like effector nucleases (TALENs) and the clustered regularly interspaced short palindromic repeat (CRISPR)/the CRISPR-associated

proteins (Cas) system. Because it is difficult to design the motif for targeted regions using ZFNs and TALENs (Carroll 2011), and requires laborious cloning steps (Joung and Sander 2013), the CRISPR/Cas system is commonly used for genome editing (Cho et al. 2013; Cong et al. 2013; Mali et al. 2013). A synthetic single-guide RNA, consisting of CRISPR RNAs and trans-activating CRISPR RNAs (Jinek et al. 2012), and Cas9 endonuclease from Streptococcus pyogenes type II are the only components essential to induce targeted DNA cleavage in rodents (Li et al. 2013a, b; Shen et al. 2013; Wang et al. 2013). A possible advantage of the CRISPR/Cas9 is the less-time consuming in the production of gene-edited animals (Mashiko et al. 2013; Yoshimi et al. 2014).

Pluripotent stem cells, such as induced pluripotent stem (iPS) cells and embryonic stem (ES) cells, are capable of compensating for developmental abnormalities in certain organ-deficient model animals. The protocol to produce developmentally compensated organs from pluripotent cells involves the injection of iPS/ES cells into blastocysts disrupted by gene-targeted mutation (Rashid et al. 2014) and would greatly contribute to the field of regenerative medicine. To date, a mouse iPS cell-derived kidney has been produced in *Sal-like 1* knockout mice (Usui et al. 2012), as well as a rat ES cell-derived thymus in *Forkhead-box N1* (*Foxn1*)$^{nu/nu}$ mice (Isotani et al. 2011) and a mouse and rat iPS cell-derived pancreas in *pancreas duodenal homeobox gene 1* (*Pdx1*) knockout mice (Kobayashi et al. 2010). In addition to blastocyst injection technology, application of somatic cell nuclear transfer technology has made it possible to produce the porcine somatic cell-derived pancreas in *Pdx1-hairy- and enhancer of split 1*-carrying transgenic pigs (Matsunari et al. 2013).

The nude phenotype in *Foxn1* gene mutants is associated with the rudimental thymus in humans (Amorosi et al. 2008; Pignata et al. 1996), mice (Flanagan 1966; Pantelouris 1968) and rats (Festing et al. 1978; Segre et al. 1995), because the *Foxn1* gene mainly regulates thymus epithelial-linage specification during organogenesis at the fetal stage (Nowell et al. 2011) and homeostasis at the postnatal stage (Brissette et al. 1996). In addition, *Foxn1* gene plays a role in skin epithelial cell maintenance at the adult stage (Lee et al. 1999; Mecklenburg et al. 2005; Meier et al. 1999). In the present study, we applied the CRISPR/Cas9 system to generate *Foxn1* mutant rats and analyzed their phenotype in terms of thymus formation, T cell population and nudity. These mutant rats, which can serve as a model valuable for thymus regenerative studies using pluripotent stem cells, were analyzed for splicing variant in thymus and skin.

Materials and methods

Preparation of Cas9 RNA and *Foxn1* single-guide RNA

The guide sequence was designed into the first exon of the rat *Foxn1* locus. Bi-cistronic expression vector px330 expressing Cas9 and single-guide RNA (Cong et al. 2013) was digested with BbsI (New England Biolabs, Ipswich, MA) and the linearized vector was gel-purified. A pair of oligonucleotides for the targeting site (Fwd: 5′-CAC CGA CTG GAG GGC GAA CCC CAA-3′, Rev: 5′-AAA CTT GGG GTT CGC CCT CCA GTC-3′) was annealed and ligated to the linearized vector. Successful insertion was confirmed by sequencing with a primer (5′-TTT GTC TGC AGA ATT GGC GC-3′). The T7 promoter was added to the Cas9 coding region by PCR amplification with a pair of primers (Fwd: 5′-TAA TAC GAC TCA CTA TAG GGA GAA TGG ACT ATA AGG ACC ACG AC-3′, Rev: 5′-GCG AGC TCT AGG AAT TCT TAC-3′). The T7-Cas9 PCR product was gel-purified and used as the template for in vitro transcription using the in vitro Transcription T7 kit (Takara Bio Inc., Shiga, Japan). The T7 promoter was also added to the *Foxn1* single-guide RNA template by PCR amplification with a pair of primers (Fwd: 5′-TTA ATA CGA CTC ACT ATA GGA CTG GAG GGC GAA CCC CAA-3′, Rev: 5′-AAA AGC ACC GAC TCG GTG CC-3′).

Co-injection of RNAs into pronuclear zygotes

All procedures for animal experimentation were reviewed and approved by the Animal Care and Use Committee of the National Institute for Physiological Sciences (Okazaki, Japan). Specific pathogen-free Wistar rats (Crlj:WI, RGD ID: 2312504) were purchased from Charles River Laboratories, Japan Inc. (Kanagawa, Japan). All rats were housed in an environmentally controlled room with a 12-h dark/12-h light cycle at a temperature of 23 ± 2 °C and

humidity of 55 ± 5 %, and given free access to a laboratory diet (CE-2; CLEA Japan Inc., Tokyo, Japan) and filtered water. Female rats at 7–8 weeks old were superovulated with 150 IU/kg equine chorionic gonadotropin (eCG; ASKA Pharmaceutical Co., Ltd., Tokyo, Japan) and 75 IU/kg human chorionic gonadotropin (hCG; ASKA Pharmaceutical Co., Ltd.) at an interval of 46–50 h. Thirty hours after hCG administration, pronuclear-stage zygotes were harvested from the females that had been mated with a fertile male rat. Cas9 RNA (either 20 or 50 ng/μL) and *Foxn1* single-guide RNA (20 ng/μL) were co-injected into a pronucleus of the zygotes. The zygotes were cultured for 16 h in modified Krebs–Ringer bicarbonate medium at 37 °C under 5 % CO_2 in air, and the survival rate of the injected zygotes and cleavage rate to the 2-cell stage were recorded. All surviving 2-cell stage embryos were transferred into oviductal ampullae of pseudopregnant rats at 0.5 day post-coitum (20–30 embryos per recipient rat).

Surveyor assay and DNA sequence analysis for target region

Genomic DNA was extracted from the mutant rat ear, and 2 μL of the genomic DNA solution (5–50 ng/μL) was mixed with 0.4 μL each of 10 μM primers specific for the *Foxn1* gene (Fwd: 5′-CAG GAC TGG GTG ATG GTG TC-3′, Rev: 5′- ACG GGG TTC CAT ATC TTG CC-3′), 10 μL of 2 × AmpliTaq Gold 360® master Mix (Life Technologies Japan, Tokyo, Japan) in 7.2 μL ultra-pure water. The mixture (20 μL) was subjected to PCR under the following conditions: 5 min at 95 °C; 35 cycle 30 s at 95 °C, 30 s at 60 °C, 40 s at 68 °C; and 68 °C for 2 min. A part of the PCR product was then denatured for 10 min at 95 °C, annealed at 2 °C/s from 95 to 85 °C, followed by step down at 0.3 °C/s from 85 to 25 °C with 1 min-holding at 85, 75, 65, 55, 45, 35 and 25 °C, and treated with Surveyor™ nuclease (Transgenomic Inc., Gaithersburg, MD) for 10 min at 95 °C, and then loaded on a 2 % (w/v) agarose gel. The other PCR products were cloned in pCR2.1 vectors using the TA cloning® kit (Invitrogen, CA, USA) and transformed into DH5α competent *Escherichia coli* (TOYOBO, Osaka, Japan). Extracted vectors were subsequently sequenced using the M13 primer by Value Read sequence service (Eurofins Genomics, Tokyo, Japan).

Peripheral lymphocytes of *Foxn1* gene-modified rats

Peripheral blood cells were collected from homozygous *Foxn1* gene-modified G2 rats (Δ44/Δ44 and Δ44/Δ60 at 8–10 weeks old; Δ60/Δ60 at 6 days old) under anesthesia with isoflurane, and the erythrocytes were hemolyzed at room temperature by 20-min treatment with red blood cell lysis solution containing 0.83 % (v/v) ammonium chloride. The blood was filtrated with nylon mesh (pore size 55 μm) and the lymphocyte cell population was stained with FITC-conjugated anti-rat CD3 (1F4, 1:100; Beckman Coulter, Tokyo, Japan), PC7-conjugated anti-rat CD45RA (OX-33, 1:100; Beckman Coulter) and PerCP-710-conjugated anti-rat CD161a (10/78, 1:100; eBioscience, Inc., San Diego, CA) for 30 min at room temperature. Each of the CD-conjugates was dissolved in 50 μL phosphate-buffered saline containing 3 % (w/v) bovine serum albumin (Sigma-Aldrich, St. Louis, MO). The CD3, CD45RA and CD161a are surface markers for T-cells, B-cells and NK-cells, respectively. The lymphocyte cell population was also stained with FITC-conjugated anti-rat CD3, PC7-conjugated anti-rat CD4 (OX-38, 1:100; Beckman Coulter) and PE-conjugated anti-rat CD8a (OX-8, 1:100; BioLegend, Inc., San Diego, CA) to identify T-cell maturation. Approximately 1×10^5 peripheral lymphocytes were analyzed by multicolor flow cytometry using a Cell Sorter SH800 (FACS: Sony Corporation, Tokyo, Japan).

5′ Rapid amplification of cDNA ends (5′ RACE) analysis

Thymus was collected from wild-type and the mutant rats at 13.5 day post-coitum. Skin was collected from wild-type and the mutant rats at 4 weeks-old. Total RNA was extracted by the RNeasy mini kit (QIAGEN Inc., Hilden, Germany) from the thymus and skin. The 5′ position of the *Foxn1* transcription products was determined by the 5′ RACE System for Rapid Amplification of cDNA Ends, Version 2.0 kit (Invitrogen) according to the manufacturer's protocol. In brief, 0.7–1 μg of total RNA was reverse-transcribed using *Foxn1* gene-specific primer (FSP)-1 (5′-GTG TGT GGG CAG GTA GAG GT-3′). The resulting cDNA were added with a poly-cytosine tail using terminal deoxynucleotidyl transferase. Then, PCR was performed with 5′ RACE abridged anchor primer to

Table 1 Generation of *Foxn1* gene-modified rats with the CRISPR/Cas9 system

Cas9 RNA (ng/μL)	Single-guide RNA (ng/μL)	No. zygotes injected	No. (%) zygotes survived	No. (%)[a] zygotes cleaved	No. zygotes transferred	No. (%) Pups born	No. (%)[a] mutants
50	20	115	87 (76)a	87 (100)	87	23 (26)	7 (30)a
20	20	80	71 (89)b	71 (100)	71	27 (38)	1 (4)b
Total		195	158 (81)	158 (100)	158	50 (32)	8 (16)

Values followed by different letters within columns denote significant differences at $p < 0.05$

[a] The percentage of cleaved zygotes and mutant pups were calculated from surviving zygotes and born pups, respectively

the poly-cytosine tail (5′-GGC CAC GCG TCG ACT AGT ACG GGI IGG GII GGG IIG-3′) and nested FSP-2 primer (5′-TGG GAG AAA GGT GTG GGT AG-3′). The second PCR was performed with a pair of abridged anchor primer (5′-GGC CAC GCG TCG ACT AGT AC-3′) and either FSP-3 (5′-AGC AAT GGG GTC TTT CCT CT-3′) or FSP-4 (5′-TAA GGG CCA TGA AGA TGA GG-3′) primer. The first and second PCR products were cloned in pCR2.1 vectors using the TA cloning kit (Invitrogen) and transformed into DH5α competent *E. coli* (TOYOBO). Extracted vectors were subsequently sequenced using the M13 primer by Value Read sequence service (Eurofins Genomics) to determine the initiation of *Foxn1* mRNA transcription.

In silico analysis of the Foxn1 protein sequence

In silico analysis of the Foxn1 protein sequence was conducted in mutant and wild-type rats. Protein sequences of mutant rats were obtained from the ApE sequence viewer (http://biologylabs.utah.edu/jorgensen/wayned/ape/) and those of wild-type Brown Norway rats (D4A1T1) and C57BL/6 mice (Q61575) were from UniProtKB (http://www.uniprot.org). All protein sequence alignments were created in CLC sequence viewer 6.6 (CLC bio Japan Inc., Tokyo, Japan).

Statistical analysis

The proportion of zygote survival, cleavage, pups born and mutants were compared by Fisher's exact probability test. FACS data regarding T-cell classification are represented as the mean + SD, and were analyzed by one-way ANOVA with the js-STAR 2.0.6j program (http://www.kisnet.or.jp/nappa/software/star/index.htm). Differences were considered to be significant at $p < 0.05$.

Results and discussion

The efficiency of generating *Foxn1* gene-modified rats by pronuclear co-injection of Cas9 RNA and single-guide RNA is shown in Table 1. Two different concentrations of Cas9 RNA (20 or 50 ng/μL) were co-injected with *Foxn1* single-guide RNA (20 ng/μL) into the pronucleus of zygotes. All surviving zygotes developed to the 2-cell stage and were transferred to recipient oviducts. The survival rate in 50 ng/μL Cas9 RNA group was slightly lower than that in 20 ng/μL Cas9 RNA group (76 vs. 89 %; $p < 0.05$), and the offspring rate in the 50 ng/μL Cas9 RNA group tended to be lower than that in the 20 ng/μL Cas9 RNA group (26 vs. 38 %; $p = 0.12$). However, the surveyor assay revealed that seven mutants (30 %) were identified from 23 newborn pups in the 50 ng/μL Cas9 RNA group, in contrast to only one mutant (4 %) from 27 pups in the 20 ng/μL Cas9 RNA group ($p < 0.05$). A total of 8 mutant rats were characterized by sequencing the 44 bp deletion (Δ44), 60 bp deletion (Δ60) or 4 bp insertion (+4) at the mono-allele of the *Foxn1* gene (Fig. 1a). Progeny analysis using three mutant founders (ID #10, #15 and #28) hypothesized that mutant ID #10 contained 75 % wild-type and 25 % Δ44, that #15 contained 87.5 % wild-type and 12.5 % Δ44, and that #28 contained 62.5 % wild-type, 12.5 % Δ44 and 25 % Δ60 (Fig. 1b). It is likely that CRISPR/Cas9-mediated genome editing occurs in rat embryos at the 2- to 4-cell stage, resulting in mosaicism of the whole body and germline. This hypothesis

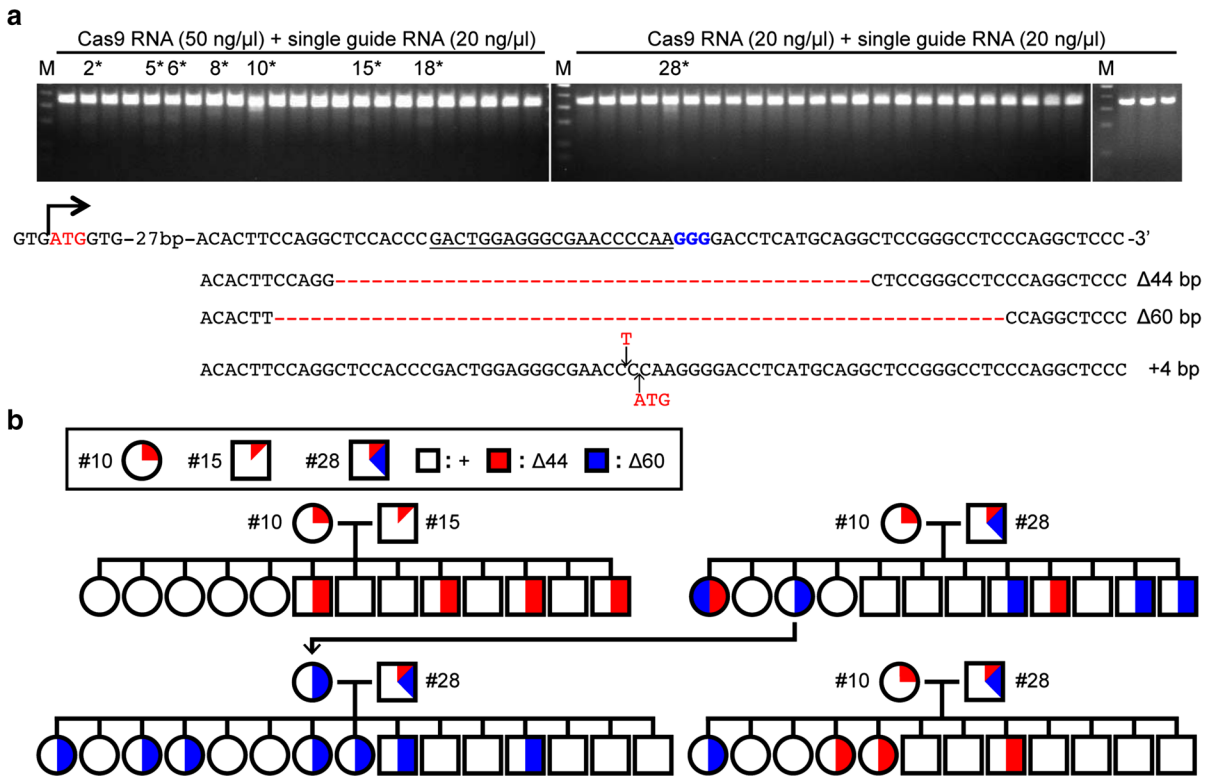

Fig. 1 Generation of *Foxn1* gene-modified rats by the CRISPR/Cas9 system. **a** Eight mutants (#2, 5, 6, 8, 10, 14, 18, 28) were identified using the surveyor assay. *Lanes 1* to *23*; Pups derived from injection of 50 ng/μL Cas9 RNA. *Lanes 24* to *50*; Pups derived from injection of 20 ng/μL Cas9 RNA. Deletion of 44 bp (Δ44) or 60 bp (Δ60), or insertion of 4 bp (+4) was found in these mutants. *M* All purpose Hi-Lo^{TM} DNA marker. *Under bar* indicates target sequence for guide RNA. PAM sequence is highlighted with *blue color*. **b** Pedigrees obtained from the sequence analyses of G0 founder and G1 progeny. (Color figure online)

corresponds with previous reports in which somatic mosaicism and allele complexity were induced by CRISPR/Cas9 RNA injections into mouse zygotes (Chapman et al. 2015; Wang et al. 2013; Yen et al. 2014). Further experiments to decrease the mosaicism are required for improvement of the CRISPR/Cas9 RNA injection protocol.

The results of G1 × G1 offspring mating (4 combinations, 5 litters: Δ44/+ × Δ44/+, Δ44/+ × Δ60/+, Δ60/+ × Δ60/+, Δ60/+ × Δ60/+, Δ44/Δ60 × Δ44/+) are summarized in Supplementary Table 1. The genotypes of G2 offspring roughly matched with Mendelian proportions, except for 2 pairs of Δ60/+ × Δ60/+ mating, suggesting that mutations of Δ44/Δ44 and Δ44/Δ60 did not affect fetal development. On the other hand, 4 G2 offspring in two litters of Δ60/+ × Δ60/+ mating were killed by cannibalism and no Δ60/Δ60 offspring were recovered at 3 weeks old. In additional Δ60/+ × Δ60/+ mating, a few dying G2 offspring appeared to be poorly developed in the lower half of the body, but analysis of the offspring failed to detect any abnormalities at post-natal day 5–6 (see Supplementary Figure 1). These offspring were found to have Δ60/Δ60 mutation. These results suggest that G2 offspring with the Δ60/Δ60 mutation were dying within 5–6 days after birth. FACS analysis of peripheral lymphocytes showed that there were few T-cells in homozygous *Foxn1* gene-modified G2 rats (Δ44/Δ44 and Δ44/Δ60 at 8–10 weeks old; Δ60/Δ60 at 6 days old) when compared with wild-type rats (Fig. 2a). Mutant rats had normal levels of B-cells and NK-cells. The proportion of peripheral T-cells in heterozygous *Foxn1* gene-modified mutants (Δ44/+: 44.1 %, Δ60/+: 34.3 %) were intermediate between that of wild-type rats (+/+: 56.9 %, $p < 0.05$) and

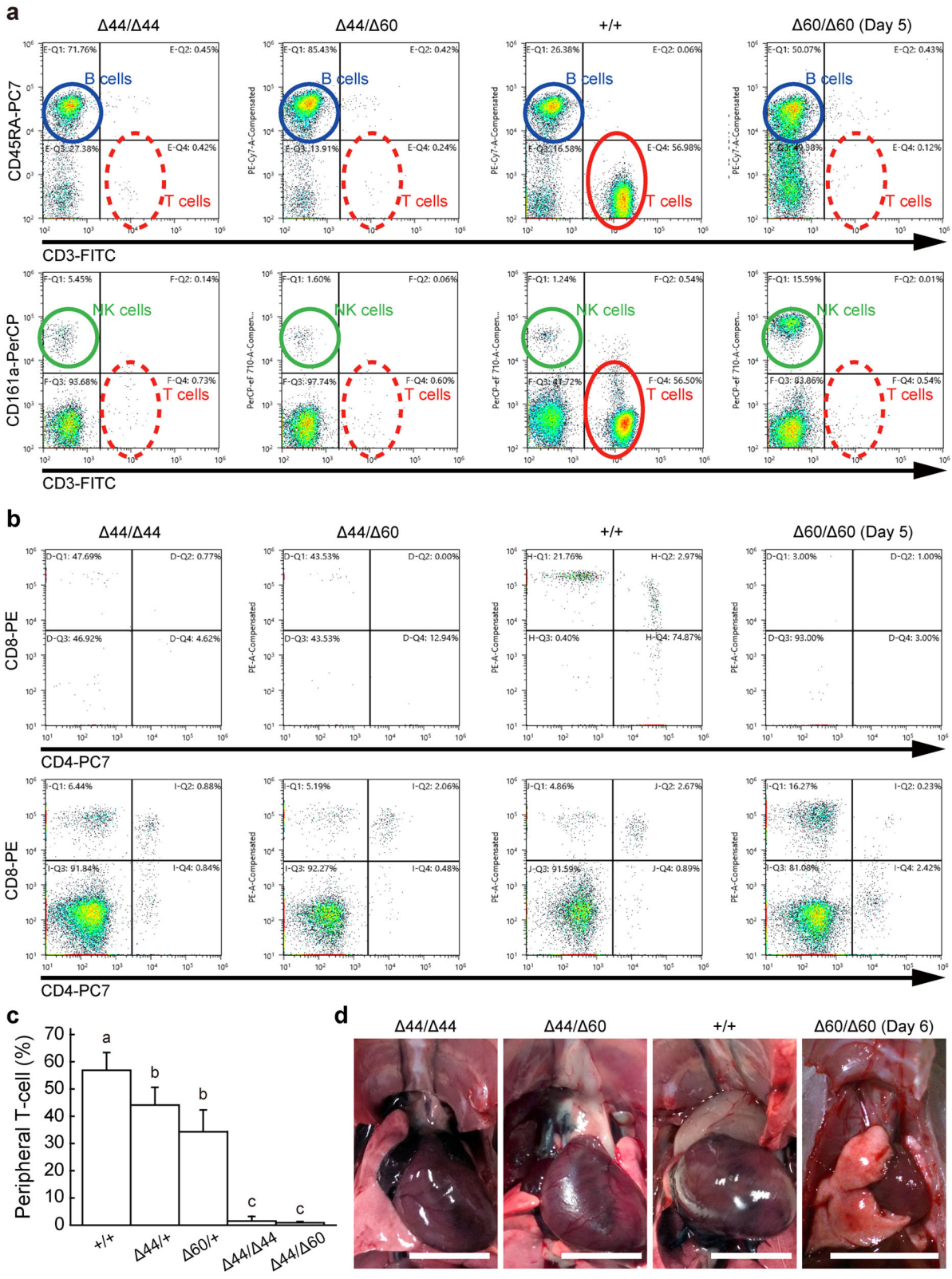
a
Δ44/Δ44
Δ44/Δ60
+/+
Δ60/Δ60 (Day 5)
CD45RA-PC7
B cells
T cells
CD3-FITC
CD161a-PerCP
NK cells
b
CD8-PE
CD4-PC7
c
Peripheral T-cell (%)
+/+
Δ44/+
Δ60/+
Δ44/Δ44
Δ44/Δ60
d
Δ44/Δ44
Δ44/Δ60
+/+
Δ60/Δ60 (Day 6)

◀**Fig. 2** Phenotype of peripheral lymphocytes and thymic organogenesis of *Foxn1* gene-modified rats (Δ44/Δ44, Δ44/Δ60 and Δ60/Δ60). **a** *Dot-plots* representing CD3-positive and CD45RA-positive population (*upper*) or CD3-positive and CD161a-positive population (*lower*). CD3-positive, CD45RA-positive and CD161a-positive cells indicate T-cells, B-cells and NK-cells, respectively. **b** *Dot-plots* representing CD4-positive and CD8a-positive cells on CD3-positive population (*upper*) or CD3-negative population (*lower*). **c** Proportion of peripheral T-cells in adult mutant rats (mean + SD). +/+; n = 6, Δ44/+; n = 5, Δ60/+; n = 7, Δ44/Δ44; n = 6, Δ44/Δ60; n = 8. *Different letters* on *SD bars* denote significant differences at $p < 0.05$. **d** Macroscopic appearance of the thymus. *Scale bar* 10 mm

homozygous *Foxn1* gene-modified mutants (Δ44/Δ44: 1.5 %, Δ44/Δ60: 1.0 %, $p < 0.05$) (Fig. 2c). Homozygous *Foxn1* gene-modified G2 rats (Δ44/Δ44 and Δ44/Δ60) at 8–10 weeks old showed thymus hypoplasia (Fig. 2d). Thymus hypoplasia was also confirmed in 5-day-old Δ60/Δ60 mutant rats. The phenotype of T-cell deficiency and thymus hypoplasia in *Foxn1* gene-modified mutant rats via the CRISPR/Cas9 system observed in the present study corresponded with the phenotype in *Foxn1*-mutant mice (Pantelouris 1968), rats (Festing et al. 1978; Vos et al. 1980) and humans (Vigliano et al. 2011). FACS analysis showed that peripheral lymphocytes with $CD4^+CD8^-$ and $CD4^+CD8^+$ on $CD3^+$ populations decreased ($p < 0.05$) in homozygous *Foxn1* gene-modified mutants rats (Δ44/Δ44: 4.6 and 0.5 %; Δ44/Δ60: 13.7 and 0.9 %, respectively) compared with heterozygous *Foxn1* gene-modified mutants (Δ44/+: 76.3 and 3.7 %; Δ60/+: 75.0 and 4.7 %, respectively) and wild-type rats (75.4 and 2.9 %, respectively; Fig. 2b). In contrast, peripheral lymphocytes with $CD4^-CD8^+$ subset increased ($p < 0.05$) in homozygous *Foxn1* gene-modified mutants rats (Δ44/Δ44: 54.4 %, Δ44/Δ60: 41.8 %) compared with heterozygous *Foxn1* gene-modified mutants (Δ44/+: 19.0 %, Δ60/+: 19.5 %) and wild-type rats (21.3 %). However, total number of $CD4^-CD8^+$ on $CD3^+$ in homozygous *Foxn1* gene-modified mutant rats was very limited. Regarding $CD3^-$ population, there were very small subsets for $CD4^+CD8^-$, $CD4^-CD8^+$ and $CD4^+CD8^+$ cells. In human, a considerable number of $CD8^+$ cells on $CD3^-$ population were reported in *FOXN1* mutant fetus (Vigliano et al. 2011).

The phenotype in hair coat during post-natal weeks 3–6 were different between the two homozygous *Foxn1* gene-modified mutant rats (Δ44/Δ44 and Δ44/Δ60), as shown in Fig. 3 and Supplementary Table 1. G2 rats with the *Foxn1* Δ44 mutations in double alleles had normal hair growth, while rats with hemi-homo Δ44/Δ60 mutations in the *Foxn1* locus exhibited a nude phenotype (Fig. 3, 4 weeks old). Interestingly, this nude phenotype was not maintained during their youth period. Cyclic alopecia was reported in *rnu* rats (Festing et al. 1978), *Mxs2* knockout mice (Ma et al. 2003) and *Sox21* knockout mice (Kiso et al. 2009). Cyclic alopecia observed in the Δ44/Δ60 mutant rat may be explained by infradian rhythm of Foxn1 expression during the hair growth cycle (Lee et al. 1999; Mecklenburg et al. 2005; Meier et al. 1999). These homozygous *Foxn1* gene-modified G2 rats were competent in their reproductive performance as they were capable of mating, delivering, and nursing,

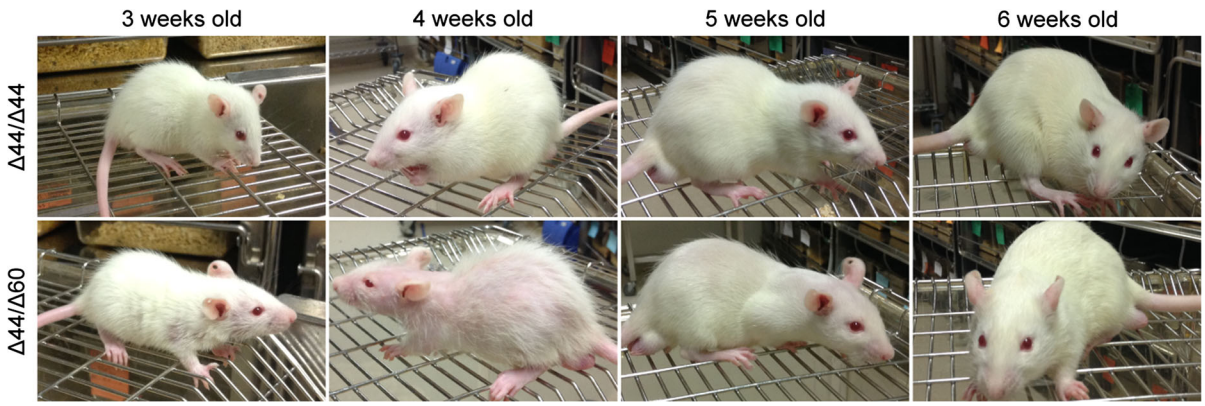

Fig. 3 Phenotype of hair coat of *Foxn1* gene-modified rats. Time-dependent change of hair coat pattern in mutant rats (*upper* Δ44/Δ44, *bottom* Δ44/Δ60)

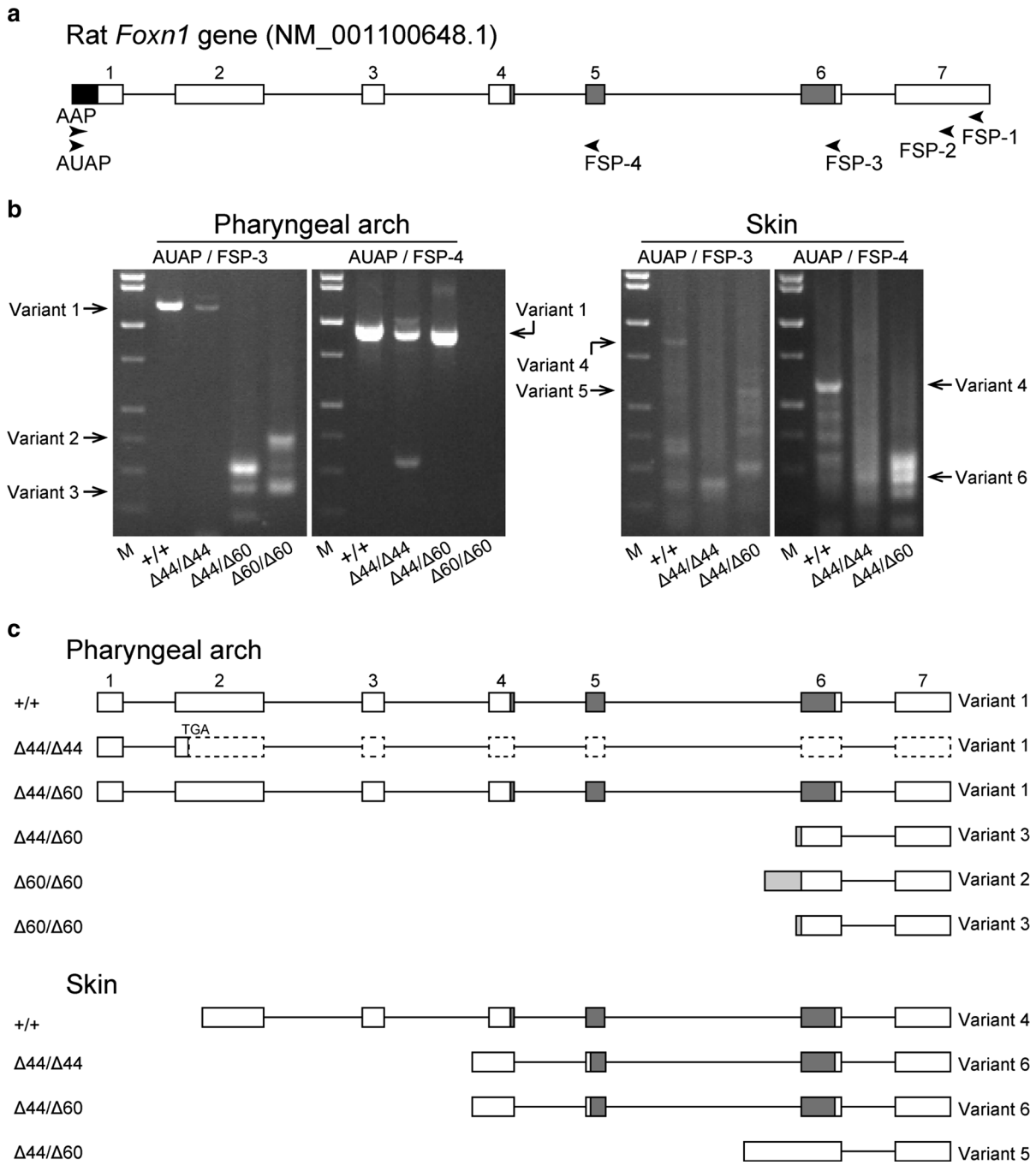

Fig. 4 Identification of *Foxn1* 5′-end and splicing variants in the pharyngeal arch and the skin of the mutant rats. **a** Schematic diagram showing locations of RACE-PCR primers used for the identification of *Foxn1* 5′-ends and splicing variants. *White boxes* and *line* represent exons and introns, respectively. DNA-binding domains are highlighted with *gray color*. Anchor sequence (*black box*) is connected upstream with 5′-ends. *Numbers on boxes* represent exon number. **b** Gel images showing major 3 variants in the pharyngeal arch and major 3 variants in the skin. *M* All purpose Hi-Lo^{TM} DNA marker. **c** Structure of 5′-end and transcriptional variants in the *Foxn1* gene determined by RACE-PCR. *Dot boxes* represent exons untranslated due to TGA stop codon. *Light gray boxes* represent sequences undefined in variants 2 and 3

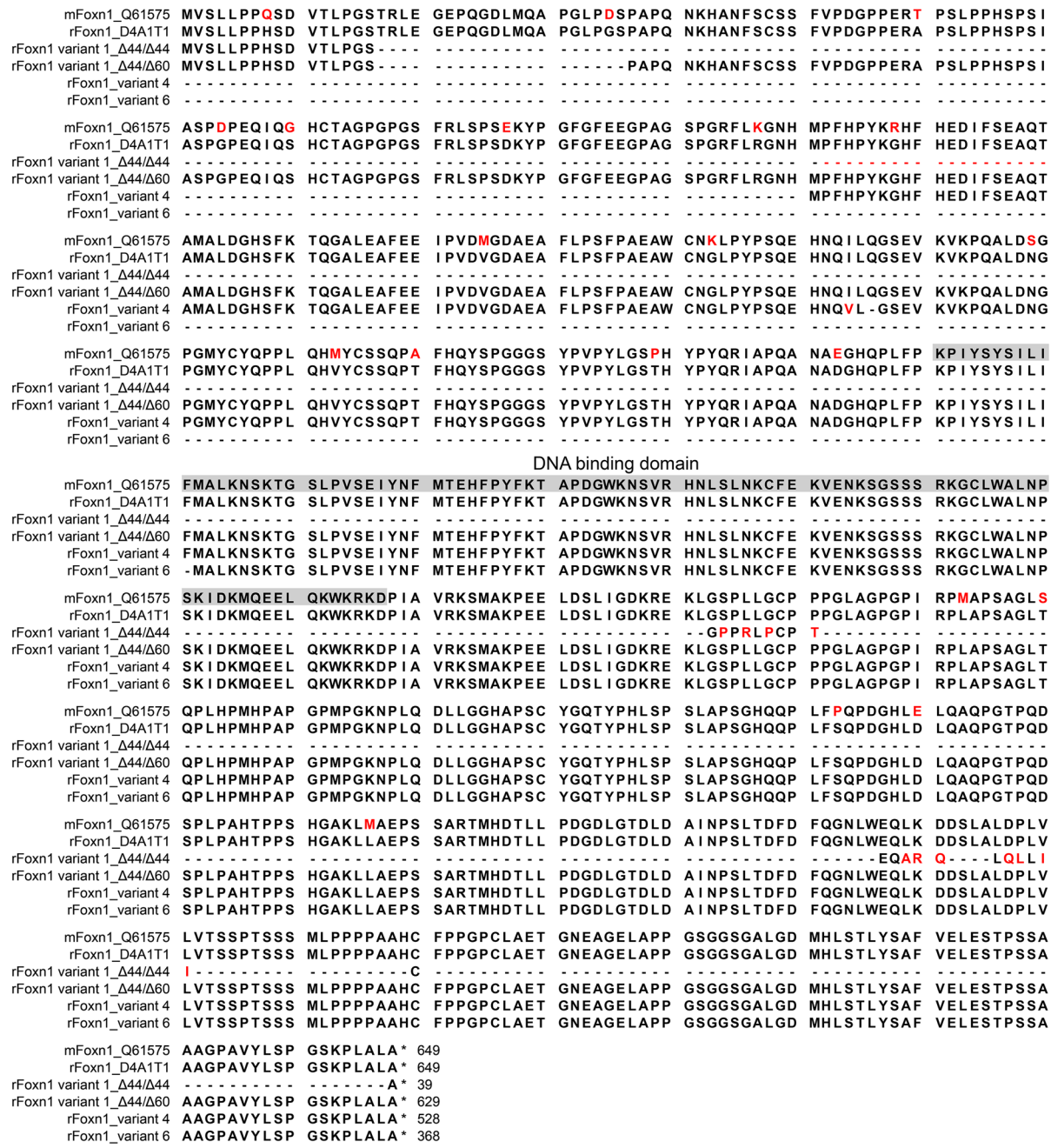

Fig. 5 In silico analysis of the Foxn1 protein sequence of each splicing variant in mutant rats (Δ44/Δ44 and Δ44/Δ60) compared to wild-type mice (Q61575) and wild-type rats (D4A1T1). The mismatch of amino acid residue and the DNA-binding domain of Foxn1 protein in the sequence are highlighted with *red* and *grey colors*, respectively. (Color figure online)

although the *rnu* rat affects not only maternal capability but also the suckling ability of the dam (Liang et al. 1997; McDermott-Lancaster et al. 1987). Thymus hypoplasia was a common phenotype among the mutants of Δ44/Δ44, Δ44/Δ60 and Δ60/Δ60, but the nude phenotype and lethality were characteristic of Δ44/Δ60 mutants and Δ60/Δ60 mutants, respectively. Additionally, there are no abnormalities in the

developmental nails and brain, which were reported to express *Foxn1* gene (Lee et al. 1999; Nehls et al. 1996). These results are corresponded with previous studies in nude mice (Meier et al. 1999).

The 5′-end of *Foxn1* transcript in the mutant rats thymus and skin was compared with the reference sequence reported previously (NM_001100648.1). The first PCR reaction was performed using a reverse FSP located on exon 7 and the forward abridged anchor primer provided by the kit. The second PCR reaction was performed using reverse FSPs located on exon 5 or 6 and the forward abridged universal anchor primer (Fig. 4a). Three each major transcription variants were identified in the pharyngeal arch and skin, respectively (Fig. 4b). Transcripts consisted of all seven exons (defined as variant 1) were found in the pharyngeal arch of wild-type, the Δ44/Δ44 mutant and the Δ44/Δ60 mutant rats (Fig. 4b, c). Transcripts without DNA-binding domain (defined as variant 2 and 3) were found in the Δ60/Δ60 mutant rats. The deletion of 44 bp leads to a frameshift and premature stop codon, resulting in the Foxn1 protein lacking the DNA-binding domain (Fig. 5). In contrast, the deletion of 60 bp leads to deletion of only the N-terminal 20 amino acids, and the DNA-binding domain is expected to function as a transcription factor. One explanation for Δ60 in variant 1 may be that folding mistake is caused by cysteine binding error. In skin, transcript without first exon (defined as variant 4) was found in wild-type rats (Fig. 4b, c). Long transcript without DNA-binding domain (defined as variant 5) was found in the Δ44/Δ60 mutant rats. Interestingly, the shorter transcripts with DNA-binding domain (defined as variant 6) were found in the Δ44/Δ44 mutant and the Δ44/Δ60 mutant rats. Normal hair growth in the Δ44/Δ44 mutant rat can be explained by the expression of short transcripts with DNA-binding domain (Fig. 5) or by complementary expression of downstream mHa3, as reported previously (Meier et al. 1999). On cyclic alopecia in the Δ44/Δ60 mutant rat, it can be speculated that amount of the two transcripts (variant 5 and 6) changes or downstream signaling compensate in hair growth stage. As to *Foxn1* gene, various types of transcripts influence its regulation pattern, as reported in *Foxn1*-edited mice (Suzuki et al. 2003; Su et al. 2003). Indeed, minor PCR products were amplified by total RNA from the skin and pharyngeal arch in the mutant rats (the Δ44/Δ60 mutant rats, especially). The *Foxn1* gene may have plasticity by the mechanism of auto-regulation and/or compensation, because this gene was reported to evolve from homologs in non-mammalian organisms that lack an anticipatory immune system (Schlake et al. 1997). Splicing variants resulting from the indel-mutation of the *Foxn1* first exon may cause hypomorphic allele. It was reported that hypomorphic allele of *Foxn1* locus was induced by lacking of exon 2 in *Foxn1*–knockout mice (Su et al. 2003).

In conclusion, *Foxn1* gene-modified mutant rats were efficiently generated by the CRISPR/Cas9 system. The mutant rats in *Foxn1* gene-edited by the CRISPR/Cas9 system showed the phenotype of thymus deficiency and incomplete hairless which was characterized by splicing variants.

Acknowledgments The authors thank Mika Douki and Keiko Yamauchi (National Institute for Physiological Sciences) for their assistance with the care and preparation of animals. This work was supported by a grant from the Japan Science and Technology Agency (JST)-Exploratory Research for Advanced Technology (ERATO)-Nakauchi Stem Cell and Organ Regeneration Project (to H.N.), a Grant-in-Aid from Japan Society for the Promotion of Science (JSPS) (No. 25290037; to M.H.) and a Grant-in-Aid from JSPS Fellows (No. 26010751; to T.G.).

Compliance with ethical standards

Conflict of interest The authors declare that they have no conflict of interest.

References

Amorosi S, D'Armiento M, Calcagno G, Russo I, Adriani M, Christiano AM, Weiner L, Brissette JL, Pignata C (2008) FOXN1 homozygous mutation associated with anencephaly and severe neural tube defect in human athymic Nude/SCID fetus. Clin Genet 73:380–384. doi:10.1111/j.1399-0004.2008.00977.x

Brissette JL, Li J, Kamimura J, Lee D, Dotto GP (1996) The product of the mouse nude locus, Whn, regulates the balance between epithelial cell growth and differentiation. Genes Dev 10:2212–2221. doi:10.1101/gad.10.17.2212

Carroll D (2011) Genome engineering with zinc-finger nucleases. Genetics 188:773–782. doi:10.1534/genetics.111.131433

Chapman KM, Medrano GA, Jaichander P, Chaudhary J, Waits AE, Nobrega MA, Hotaling JM, Ober C, Hamra FK (2015) Targeted germline modifications in rats using CRISPR/Cas9 and spermatogonial stem cells. Cell Rep 10:1828–1835. doi:10.1016/j.celrep.2015.02.040

Cho SW, Kim S, Kim JM, Kim JS (2013) Targeted genome engineering in human cells with the Cas9 RNA-guided

endonuclease. Nat Biotechnol 31:230–232. doi:10.1038/nbt.2507

Cong L, Ran FA, Cox D, Lin S, Barretto R, Habib N, Hsu PD, Wu X, Jiang W, Marraffini LA, Zhang F (2013) Multiplex genome engineering using CRISPR/Cas systems. Science 339:819–823. doi:10.1126/science.1231143

Festing MF, May D, Connors TA, Lovell D, Sparrow S (1978) An athymic nude mutation in the rat. Nature 274:365–366. doi:10.1038/274365a0

Flanagan SP (1966) 'Nude', a new hairless gene with pleiotropic effects in the mouse. Genet Res 8:295–309. doi:10.1017/S0016672300010168

Isotani A, Hatayama H, Kaseda K, Ikawa M, Okabe M (2011) Formation of a thymus from rat ES cells in xenogeneic nude mouse‹ ›rat ES chimeras. Genes Cells 16:397–405. doi:10.1111/j.1365-2443.2011.01495.x

Jinek M, Chylinski K, Fonfara I, Hauer M, Doudna JA, Charpentier E (2012) A programmable dual-RNA-guided DNA endonuclease in adaptive bacterial immunity. Science 337:816–821. doi:10.1126/science.1225829

Joung JK, Sander JD (2013) TALENs: a widely applicable technology for targeted genome editing. Nat Rev Mol Cell Biol 14:49–55. doi:10.1038/nrm3486

Kiso M, Tanaka S, Saba R, Matsuda S, Shimizu A, Ohyama M, Okano HJ, Shiroishi T, Okano H, Saga Y (2009) The disruption of Sox21-mediated hair shaft cuticle differentiation causes cyclic alopecia in mice. Proc Natl Acad Sci USA 106:9292–9297. doi:10.1073/pnas.0808324106

Kobayashi T, Yamaguchi T, Hamanaka S, Kato-Itoh M, Yamazaki Y, Ibata M, Sato H, Lee YS, Usui J, Knisely AS, Hirabayashi M, Nakauchi H (2010) Generation of rat pancreas in mouse by interspecific blastocyst injection of pluripotent stem cells. Cell 142:787–799. doi:10.1016/j.cell.2010.07.039

Lee D, Prowse DM, Brissette JL (1999) Association between mouse nude gene expression and the initiation of epithelial terminal differentiation. Dev Biol 208:362–374. doi:10.1006/dbio.1999.9221

Li D, Qiu Z, Shao Y, Chen Y, Guan Y, Liu M, Li Y, Gao N, Wang L, Lu X, Zhao Y, Liu M (2013a) Heritable gene targeting in the mouse and rat using a CRISPR-Cas system. Nat Biotechnol 31:681–683. doi:10.1038/nbt.2661

Li W, Teng F, Li T, Zhou Q (2013b) Simultaneous generation and germline transmission of multiple gene mutations in rat using CRISPR-Cas systems. Nat Biotechnol 31:684–686. doi:10.1038/nbt.2652

Liang SC, Lin SZ, Yu JF, Wu SF, Wang SD, Liu JC (1997) F344-rnu/rnu athymic rats: breeding performance and acceptance of subcutaneous and intracranial xenografts at different ages. Lab Anim Sci 47:549–553

Ma L, Liu J, Wu T, Plikus M, Jiang TX, Bi Q, Liu YH, Muller-Rover S, Peters H, Sundberg JP, Maxson R, Maas RL, Chuong CM (2003) 'Cyclic alopecia' in Msx2 mutants: defects in hair cycling and hair shaft differentiation. Development 130:379–389. doi:10.1242/dev.00201

Mali P, Yang L, Esvelt KM, Aach J, Guell M, DiCarlo JE, Norville JE, Church GM (2013) RNA-guided human genome engineering via Cas9. Science 339:823–826. doi:10.1126/science.1232033

Mashiko D, Fujihara Y, Satouh Y, Miyata H, Isotani A, Ikawa M (2013) Generation of mutant mice by pronuclear injection of circular plasmid expressing Cas9 and single guided RNA. Sci Rep 3:3355. doi:10.1038/srep03355

Matsunari H, Nagashima H, Watanabe M, Umeyama K, Nakano K, Nagaya M, Kobayashi T, Yamaguchi T, Sumazaki R, Herzenberg LA, Nakauchi H (2013) Blastocyst complementation generates exogenic pancreas in vivo in apancreatic cloned pigs. Proc Natl Acad Sci USA 110:4557–4562. doi:10.1073/pnas.1222902110

McDermott-Lancaster RD, Ito T, Kohsaka K, Colston MJ (1987) The nude mouse-characteristics, breeding and husbandry. Int J Lepr Other Mycobact Dis 55:885–888

Mecklenburg L, Tychsen B, Paus R (2005) Learning from nudity: lessons from the nude phenotype. Exp Dermatol 14:797–810. doi:10.1111/j.1600-0625.2005.00362.x

Meier N, Dear TN, Boehm T (1999) Whn and mHa3 are components of the genetic hierarchy controlling hair follicle differentiation. Mech Dev 89:215–221. doi:10.1016/S0925-4773(99)00218-X

Nehls M, Kyewski B, Messerle M, Waldschutz R, Schuddekopf K, Smith AJ, Boehm T (1996) Two genetically separable steps in the differentiation of thymic epithelium. Science 272:886–889. doi:10.1126/science.272.5263.886

Nowell CS, Bredenkamp N, Tetelin S, Jin X, Tischner C, Vaidya H, Sheridan JM, Stenhouse FH, Heussen R, Smith AJ, Blackburn CC (2011) Foxn1 regulates lineage progression in cortical and medullary thymic epithelial cells but is dispensable for medullary sublineage divergence. PLoS Genet 7:e1002348. doi:10.1371/journal.pgen.1002348

Pantelouris EM (1968) Absence of thymus in a mouse mutant. Nature 217:370–371. doi:10.1038/217370a0

Pignata C, Fiore M, Guzzetta V, Castaldo A, Sebastio G, Porta F, Guarino A (1996) Congenital Alopecia and nail dystrophy associated with severe functional T-cell immunodeficiency in two sibs. Am J Med Genet 65:167–170. doi:10.1002/(SICI)1096-8628(19961016)65:2<167:AID-AJMG17>3.0.CO;2-O

Rashid T, Kobayashi T, Nakauchi H (2014) Revisiting the flight of Icarus: making human organs from PSCs with large animal chimeras. Cell Stem Cell 15:406–409. doi:10.1016/j.stem.2014.09.013

Schlake T, Schorpp M, Nehls M, Boehm T (1997) The nude gene encodes a sequence-specific DNA binding protein with homologs in organisms that lack an anticipatory immune system. Proc Natl Acad Sci USA 94:3842–3847

Segre JA, Nemhauser JL, Taylor BA, Nadeau JH, Lander ES (1995) Positional cloning of the nude locus: genetic, physical, and transcription maps of the region and mutations in the mouse and rat. Genomics 28:549–559. doi:10.1006/geno.1995.1187

Shen B, Zhang J, Wu H, Wang J, Ma K, Li Z, Zhang X, Zhang P, Huang X (2013) Generation of gene-modified mice via Cas9/RNA-mediated gene targeting. Cell Res 23:720–723. doi:10.1038/cr.2013.46

Su DM, Navarre S, Oh WJ, Condie BG, Manley NR (2003) A domain of Foxn1 required for crosstalk-dependent thymic epithelial cell differentiation. Nat Immunol 4:1128–1135. doi:10.1038/ni983

Suzuki N, Hirata M, Kondo S (2003) Traveling stripes on the skin of a mutant mouse. Proc Natl Acad Sci 100:9680–9685. doi:10.1073/pnas.1731184100

Usui J, Kobayashi T, Yamaguchi T, Knisely AS, Nishinakamura R, Nakauchi H (2012) Generation of kidney from pluripotent stem cells via blastocyst complementation. Am J Pathol 180:2417–2426. doi:10.1016/j.ajpath.2012.03.007

Vigliano I, Gorrese M, Fusco A, Vitiello L, Amorosi S, Panico L, Ursini MV, Calcagno G, Racioppi L, Del Vecchio L, Pignata C (2011) FOXN1 mutation abrogates prenatal T-cell development in humans. J Med Genet 48:413–416. doi:10.1136/jmg.2011.089532

Vos JG, Kreeftenberg JG, Kruijt BC, Kruizinga W, Steerenberg P (1980) The athymic nude rat. II. Immunological characteristics. Clin Immunol Immunopathol 15:229–237. doi:10.1016/0090-1229(80)90033-1

Wang H, Yang H, Shivalila CS, Dawlaty MM, Cheng AW, Zhang F, Jaenisch R (2013) One-step generation of mice carrying mutations in multiple genes by CRISPR/Cas-mediated genome engineering. Cell 153:910–918. doi:10.1016/j.cell.2013.04.025

Yen ST, Zhang M, Deng JM, Usman SJ, Smith CN, Parker-Thornburg J, Swinton PG, Martin JF, Behringer RR (2014) Somatic mosaicism and allele complexity induced by CRISPR/Cas9 RNA injections in mouse zygotes. Dev Biol 393:3–9. doi:10.1016/j.ydbio.2014.06.017

Yoshimi K, Kaneko T, Voigt B, Mashimo T (2014) Allele-specific genome editing and correction of disease-associated phenotypes in rats using the CRISPR-Cas platform. Nat Commun 5:4240. doi:10.1038/ncomms5240